MATEC Web of Conferences **1**, 10005 (2012)
DOI: 10.1051/matecconf/20120110005

Nonlinear Dynamic Response of Compliant Journal Bearings

M. Cha[1], and S. Glavatskih[1,2]

[1]The Royal Institute of Technology, Department of Machine Design, 100 44 Stockholm, Sweden
[2]Ghent University, Department of Mechanical Construction and Production, 9000 Ghent, Belgium

Abstract. This paper investigates the dynamic response of the compliant tilting pad journal bearings subjected to synchronous excitation. Bearing compliance is affected by the properties of pad liner and pad support geometry. Different unbalance eccentricities are considered. It is shown that bearing dynamic response is non-linear. Journal orbit complexity increases with pad compliance though the orbit amplitudes are marginally affected at low loads. At high loads, the journal is forced to operate outside the bearing clearance. The polymer liner reduces the maximum oil film pressure by a factor of 2 when compared to the white metal liner. The nonlinear dynamic response of compliant tilting pad journal bearings is thoroughly discussed.

1 Introduction

Hydrodynamic journal bearings are widely used to support rotors in large rotating machinery such as turbines, electric motors, generators, and pumps. Lubricant, usually turbine oil, is dragged by the rotor into the contact between the bearing and rotor surfaces. This process results in the formation of a hydrodynamic lubricant film that separates the rotor from the bearing and provides very low friction. No wear occurs as long as the rotor rotates. Frequent start-ups and shut-downs may lead to excessive wear since few micrometres thick film is not maintained. Film breakdown may also occur at large amplitude rotor motion due to an excessive dynamic load.

Hydrodynamic journal bearings are preferred to rolling element bearings due to better damping characteristics and split design. In the tilting pad journal bearings, pads can independently tilt in the circumferential direction improving dynamic characteristics compared to the fixed geometry bearings. If the pad support geometry is modified to the ball-socket pivot, the pads can also tilt in the axial direction. This minimises the effect of rotor misalignment.

The pads are traditionally lined with white metal, soft alloy, to prevent rotor damage during start-ups and shut-downs. White metal also prevents rotor surface damage caused by hard, abrasive particles that may be present in the oil due to contamination. The particles are easily embedded into the white metal. At high start-up loads, a hydrostatic system is usually used to lift the rotor and prevent damage by separating bearing and journal surfaces. Tribological properties of the bearings are improved by the implementation of the polymer liners. A polymer composite liner based on polytetrafluoroethylene (PTFE) significantly reduces break-away friction compared to the white metal [1]. It was also shown that PTFE can improve steady state operating characteristics of a plain cylindrical journal bearing. PTFE makes the bearing compliant, which increases the oil film thickness and load carrying capacity. It also reduces the maximum oil film pressure by up to 40% compared to the white metal bearings [2]. The dynamic response of plain compliant bearings is similar to the white metal bearings at low dynamic loads [3]. At high dynamic loads, the journal amplitudes in the compliant bearings are larger due to the polymer liner deformation. Larger journal amplitudes can also be expected in the tilting pad journal bearings compared to plain bearings. The increase is due to the design of tilting pads. The implementation of the polymer liner on the load carrying side of the tilting pads may further increase the compliance of the bearing and consequently journal orbits. No publications dealing with the analyses of steady state or dynamic performance of compliant tilting pad journal bearings are available.

This paper investigates the dynamic response of compliant tilting pad journal bearings subjected to a synchronous excitation force. Since large deformations are expected due to the polymer liner in combination with high dynamic forces, the nonlinear analysis is employed to accurately model the bearing dynamic response.

2 Numerical model

A rigid rotor is supported by two identical journal bearings. Due to the symmetry of the rotor-bearing system, we consider only one bearing. A cross-sectional view of a tilting pad journal bearing lubricated by

Newtonian, incompressible, isoviscous fluid is shown in Figure 1. Laminar lubricant flow is assumed.

The oil film reaction forces are calculated by integrating hydrodynamic pressure over the bearing surface. The time dependent Reynolds equation is written as follows:

$$\frac{1}{R^2}\frac{\partial}{\partial\theta}\left(\frac{h^3}{\mu}\frac{\partial p}{\partial\theta}\right)+\frac{\partial}{\partial z}\left(\frac{h^3}{\mu}\frac{\partial p}{\partial z}\right)=6\Omega\frac{\partial h}{\partial\theta}+12\frac{\partial h}{\partial t} \quad (1)$$

where p is the oil film pressure, Ω is the rotor angular speed, and μ is the oil dynamic viscosity. The oil film thickness, h, is given by:

$$h(\theta)=C_p-(C_p-C_b)\cos(\theta-\psi_i)-(R+d)\delta_i\sin(\theta-\psi_i) + x\cos(\theta)+y\sin(\theta)+\delta_r(\theta) \quad (2)$$

where ψ_i is the angular pivot location, δ_i is the pad initial tilt angle and δ_r is the pad and liner deformation. The motion of the journal mass centre is given as follows:

$$M\ddot{x}=F_x+M\xi\Omega^2\cos(\Omega t)+W \quad (3)$$
$$M\ddot{y}=F_y+M\xi\Omega^2\sin(\Omega t)$$

where M is the journal mass, W is the static load, F_x, F_y are the oil film reaction forces and ξ is the unbalance eccentricity. Unbalance eccentricity is created when the mass centre of the rotor does not coincide with its geometrical centre. $M\xi\Omega^2$ is the unbalance force. The Reynolds equation, equations of motion and pad deformation are solved simultaneously until the final journal orbits are obtained [4]. The numerical model has been verified by comparing with the published data for the white metal bearings [5]. A good agreement was obtained.

3 Results

Rotor motion in the tilting pad journal bearing, Figure 1, is presented for the static load of 30kN, and the rotor angular speed of 3000 rpm. The unbalance eccentricities of $100\mu m$ and $300\mu m$ are considered. The results are given for the bearings with the line and ball-socket pivot pads. Influence of white metal and polymer composite liners on bearing response to the excitation force is shown. Table 1 presents material properties and bearing specification.

3.1. White Metal Liner

We first consider an unbalance eccentricity of $100\mu m$ which represents a small dynamic load (33% of the static load). Figure 2 shows the journal orbits in the bearings with the line and ball-socket pivot pads. Relative journal displacements in the x and y directions are shown along the X- and Y- axes. The journal displacements are made non-dimensional by dividing them by the pad radial clearance, C_p.

The line pivot pads provide much smaller orbit than the ball-socket pivot pads. The difference is due to the larger deformation of the ball-socket pivot pads in the axial direction. Larger deformation also results in increased journal eccentricity. Since the dynamic load is small (less than the static load), the orbit resemble an oval shape with an additional pole. The journal mass centre is forced in between the pads creating these three poles. Since the dynamic force is small, two upper poles are somewhat obscure.

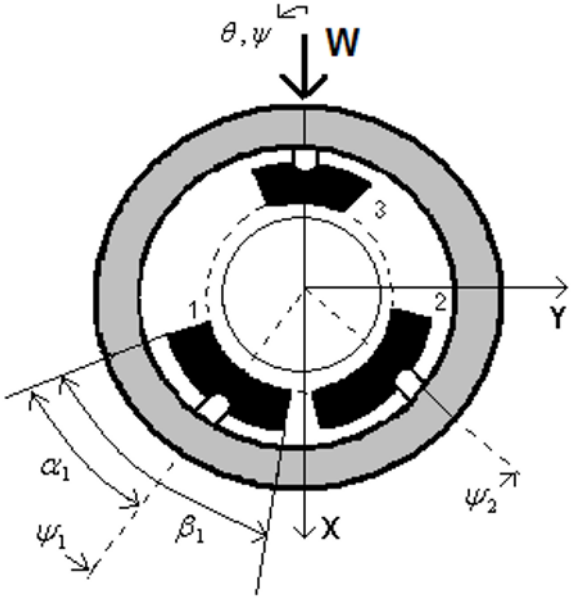

Fig. 1. Bearing geometry.

Table 1. Material properties and bearing specification.

Journal radius, R	60 [mm]
Pad thickness, d	30 [mm]
Bearing length, L	72 [mm]
Bearing radial clearance, C_b	60 [μm]
Pad radial clearance, C_p	120 [μm]
Pad angle	$\beta_1=80$; $\beta_2=80$; $\beta_3=60$
Pivot positions in the bearing	$\psi_1=130$; $\psi_1=230$; $\psi_3=0$
Pad pivot position	$\alpha_i/\beta_i=0.56$
Lubricant viscosity, μ	0.013 [Pas]
Young's modulus, E_{Steel} Young's modulus, E_{PTFE}	200 [GPa] 0.11 [GPa]
Poisson's ratio, ν_{Steel} Poisson's ratio, ν_{PTFE}	0.33 0.46
Journal mass, M	1000 [kg]

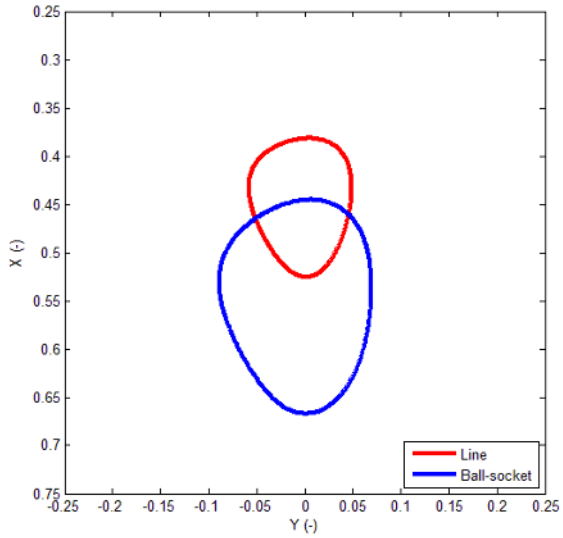

Fig. 2. White metal bearings, small dynamic load.

Now we consider a case with the unbalance eccentricity of $300\mu m$ which corresponds to 100% of the static load. Figure 3 shows the comparison of the journal orbits in the bearings with the line and ball-socket pivot pads. Numbers with arrows represent time in seconds.

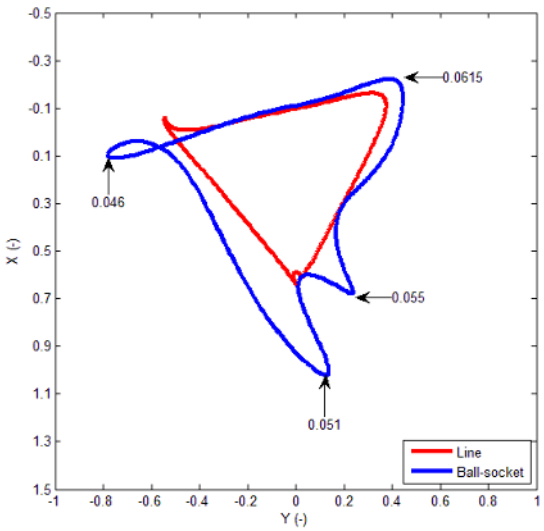

Fig. 3. White metal bearings, large dynamic load.

Once again, we can observe a smaller orbit provided by the line pivot pads compared to the ball-socket pivot pads. The shape is triangular since there are three pads in the bearing. Two bottom pads are heavily loaded whereas the upper pad is lightly loaded. Higher compliance of the ball-socket pivot pads allows the journal to be pushed much deeper in between the pads 1 and 2 (0.051s). A small peak located near the bottom corner of the orbit (red colour) for the line pivot pads is amplified when the ball-socket pivot pads (blue colour) are introduced (0.055s). The rotating journal moves counter-clockwise along the orbit. But at 0.046s it moves clockwise producing a loop. Such behaviour is explained in the Discussion section.

3.2 Polymer liner

Thickness of the polymer liner applied to the pads is 1mm. Figure 4 shows journal orbits in the compliant bearings for the small dynamic load. The orbits produced are similar in size, shape and position.

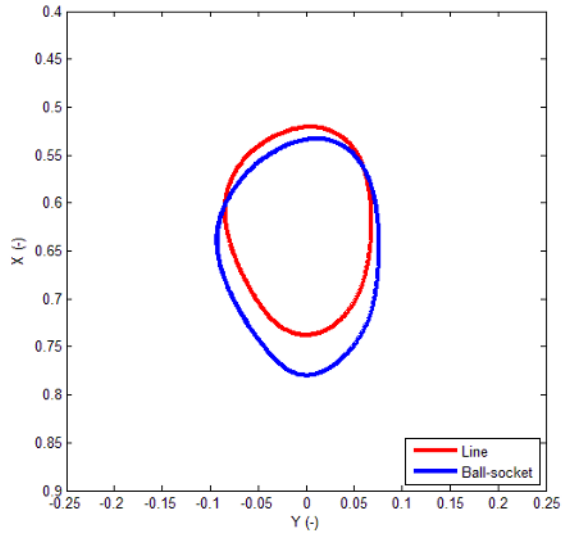

Fig. 4. Polymer lined bearings, small dynamic load.

But the polymer liner increases the journal orbit size in both X and Y directions. The journal eccentricities are also higher, see for comparison Figure 2. Polymer liner deformation is dominant being larger than pad backing deformation. This explains similarity of the orbits for both pad support geometries.

Large dynamic load significantly changes bearing response, Figure 5. The journal orbits in the line and ball-socket pivot pads have similar positions and size but the shape becomes more complex.

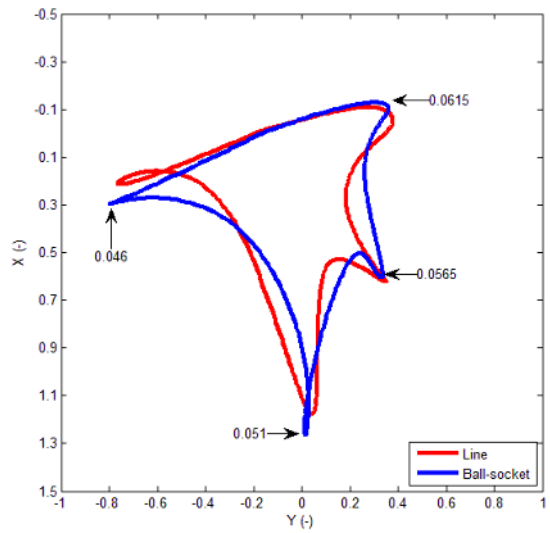

Fig. 5. Polymer lined bearings, large dynamic load.

Amplitudes of the journal motion in the x and y directions are high. The journal is forced deep in between lower pads, crossing the circle of the radial clearance.

4 Discussion

The ball-socket pivot pads with traditional white metal liner always result in larger orbit size compared to the line pivot pads under both small and large dynamic loads. Their higher compliance is responsible for the larger size and more complex shape of the orbit. Looking at Figure 3, the differences are the loop at the left corner (0.046s) and the amplified peak near the bottom corner of the orbit (0.055s). In order to further investigate these differences, the evolution of the maximum oil film pressure on each pad is analysed, Figure 6.

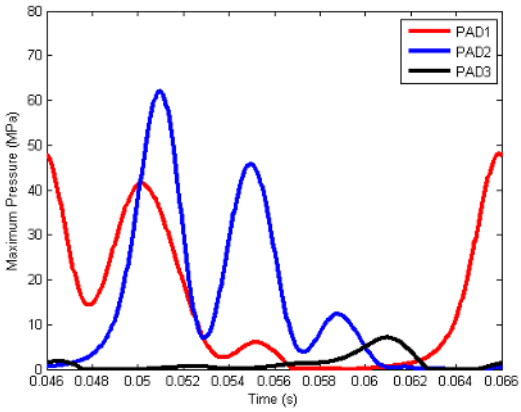

Fig. 6. Ball-socket pivot pads, white metal liner.

The journal reaches its dynamic equilibrium state after 0.03s. At 0.046s (Figure 6), the journal is located at the left corner of the orbit (Figure 3). At this time instance, pad 3 is almost unloaded while pad 1 is loaded. High oil film pressure of pad 1 lifts the journal up as it rotates counter-clockwise. The journal moves clockwise creating the loop shape path. The load is then gradually shifted from pad 1 to pad 2 smoothly forcing the journal to the bottom corner of the orbit at 0.051s. Since the oil film pressure on pad 2 is high, the journal cannot follow along pad 2 surface. The journal is then pushed in the opposite direction and as it moves away from pad 2, a diverging gap is formed. Oil film pressure on pad 2 drops and the journal falls back at 0.055s. This motion forms then converging geometry, increases oil film pressure and lifts the journal up. Pad 2 becomes gradually less loaded, while pad 1 becomes loaded pushing the journal to the left at 0.0615s.

With the polymer liner, bearings with both pad pivot geometries show similar dynamic response (Figure 5). The difference is in the location of the loop. It is at the left corner of the orbit for the line pivot pads (red colour) whereas for the ball-socket pivot pads (blue colour), it is located at the bottom corner of the orbit. Formation of the loop in the journal path in the line pivot pads with the polymer liner can be explained in a similar way as in the case of the ball-socket pivot pads with traditional white metal liner.

Figure 7 presents the variation of the maximum oil film pressure for the ball-socket pivot pads with the polymer liner. There is no loop at the left corner of the orbit at 0.046s as the oil film pressure is not high enough (as compared to Figure 6, pad 1) to lift up the journal. At 0.051s, pad 2 is more loaded than pad 1. Higher oil film pressure at pad 2 pushes the journal to the left, to the lower pressure region at pad 1. The dynamic load decreases with time and the rotor moves upwards forming the loop (blue colour).

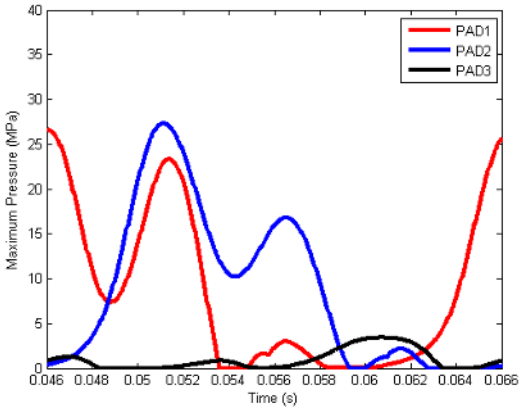

Fig. 7. Ball-socket pivot pads, polymer liner.

For a bearing designer the following observations are of importance: the polymer liner reduces the maximum oil film pressure by a factor of 2 compared to the white metal liner; both ball-socket pivot pads with white metal and line pivot pads with polymer liner force the journal to move along similar orbits. Bearing dynamic performance can be adjusted by selecting more or less elastic polymers (like e.g. PEEK).

5 Conclusion

A comparative analysis of the white metal and polymer lined tilting pad journal bearings subjected to a static load and unbalance force shows that they provide nonlinear dynamic response. Journal orbit complexity increases with pad compliance though the orbit amplitudes are marginally affected at low loads. At high loads, the journal is forced to operate outside the bearing clearance.

Acknowledgements

Financial support provided by the Swedish Hydropower Centre (SVC) is gratefully acknowledged. SVC has been established by the Swedish Energy Agency, Elforsk and Svenska Kraftnät in partnership with academic institutions.

References

1. A. Golchin, G.F. Simmons, S.B. Glavatskih, Tribology Int. (2011) doi: 10.1016/j.triboint.2011.03.025
2. E. Kuznetsov, S.B. Glavatskih, M. Fillon. Tribology Int, **44** (2011) doi:10.1016/j.triboint.2011.05.013
3. M. Cha, E. Kuznetsov, S.B. Glavatskih, Mechanisms and Machine Theory. (submitted, 2011)
4. COMSOL Multiphysics User's Guide, Version 3.5a (2008)
5. H. Desbordes, M. Fillon, C. Chan Hew Wai. J. of Tribology, **117** (1995)